Global Insights Into Lysine Acylomes Reveal Crosstalk Between Lysine Acetylation and Succinylation in *Streptomyces coelicolor* Metabolic Pathways

Authors

Yujiao Yang, Hong Zhang, Zhenyang Guo, Siwei Zou, Fei Long, Jiacheng Wu, Peng Li, Guo-ping Zhao, and Wei Zhao

Correspondence

lipeng4754@163.com; gpzhao@sibs.ac.cn; wei.zhao1@siat.ac.cn

Graphical Abstract

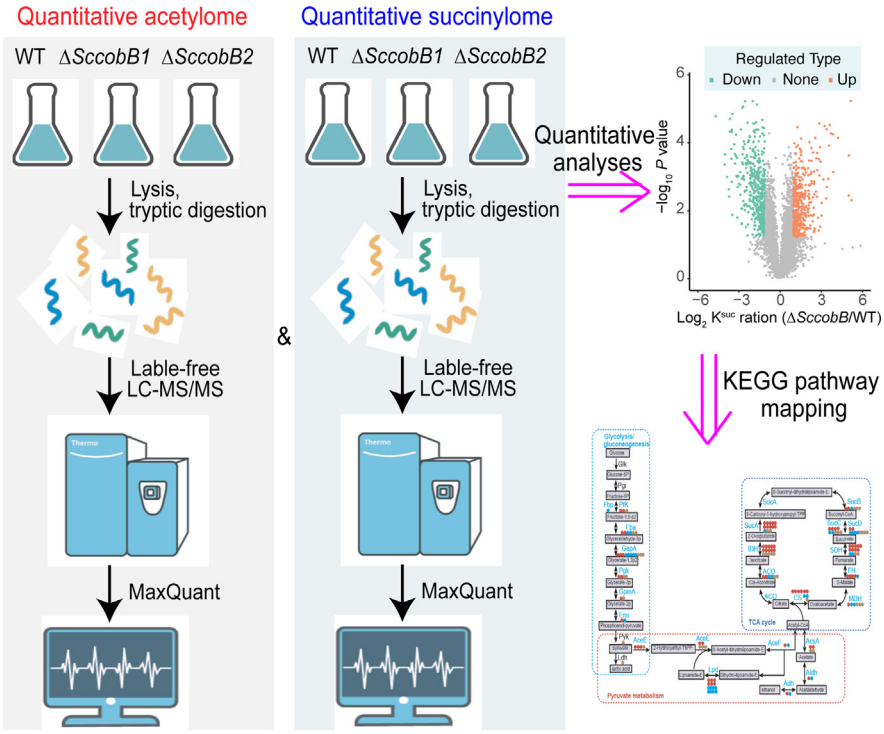

In Brief

The bimodification of lysine acylation has been observed in multiple organisms, while the understanding of acylation crosstalk remains at an early stage. In the current study, by implementing proteome-wide analyses, an extensive overlap of lysine acetylation and succinylation was revealed in *S. coelicolor*. Moreover, the modification sites were quantified by knocking out either the deacetylase *Sc*CobB1 or the desuccinylase *Sc*CobB2, demonstrating a possible competitive relationship between the acetylation and succinylation *in vivo*. Further analyses suggested that these bimodification proteins were enriched in multiple metabolic pathways including the tricarboxylic acid cycle and protein translation pathways.

Highlights

- A highly abundant and dynamic acetylation is discovered in *Streptomyces coelicolor.*
- Quantitative acetylome and succinylome analyses in *Streptomyces coelicolor*.
- The bimodification proteins are enriched in multiple metabolic pathways.

2021, Mol Cell Proteomics *20*, 100148

https://doi.org/10.1016/j.mcpro.2021.100148

Global Insights Into Lysine Acylomes Reveal Crosstalk Between Lysine Acetylation and Succinylation in *Streptomyces coelicolor* Metabolic Pathways

Yujiao Yang[1,2,3,‡], Hong Zhang[1,‡], Zhenyang Guo[4], Siwei Zou[2], Fei Long[2], Jiacheng Wu[1,3], Peng Li[4,*], Guo-ping Zhao[1,2,3,*], and Wei Zhao[2,*]

Lysine acylations are reversible and ubiquitous post-translational modifications that play critical roles in regulating multiple cellular processes. In the current study, highly abundant and dynamic acetylation, besides succinylation, was uncovered in a soil bacterium, *Streptomyces coelicolor*. By affinity enrichment using anti–acetyl-lysine antibody and the following LC–MS/MS analysis, a total of 1298 acetylation sites among 601 proteins were identified. Bioinformatics analyses suggested that these acetylated proteins have diverse subcellular localization and were enriched in a wide range of biological functions. Specifically, a majority of the acetylated proteins were also succinylated in the tricarboxylic acid cycle and protein translation pathways, and the bimodification occurred at the same sites in some proteins. The acetylation and succinylation sites were quantified by knocking out either the deacetylase *Sc*CobB1 or the desuccinylase *Sc*CobB2, demonstrating a possible competitive relationship between the two acylations. Moreover, *in vitro* experiments using synthetically modified peptides confirmed the regulatory crosstalk between the two sirtuins, which may be involved in the collaborative regulation of cell physiology. Collectively, these results provided global insights into the *S. coelicolor* acylomes and laid a foundation for characterizing the regulatory roles of the crosstalk between lysine acetylation and succinylation in the future.

The reversible protein post-translational modifications (PTMs) such as acetylation and succinylation function as efficient regulatory mechanisms that fine-tune protein activity, stability, subcellular localization, and others (1, 2). Among the 20 amino acid residues in proteins, lysine (K) is one of the most frequent targets for different PTMs. With the rapid development of high-resolution MS and immunoaffinity purification technology, diverse acylations on lysine, including acetylation (3, 4), succinylation (5), malonylation (6), glutarylation (7), propionylation (8), butyrylation (8), and lactylation (9), have been discovered in the past decade.

N-ε-Lysine acylation consists of two reversible reactions—the acylation, in which the acyl groups are added to the ε-amino of lysine residues by specific acyltransferases (2) or nonenzymatic reactions (10), and the deacylation, which is the removal of the acyl groups from the acylated proteins by deacylases (11, 12). The deacylations by sirtuins play dominant regulatory roles in cell physiology. Seven sirtuins (SIRT1–SIRT7) were identified in human cells that modulate multiple cellular processes (13), whereas only one sirtuin (CobBL) was reported in *Escherichia coli* as a bifunctional deacetylase and desuccinylase (14).

Acetylation among different acylations is one of the most well-studied lysine modifications that has gained increasing attentions. It has been reported to be involved in the regulation of multiple cellular processes, like gene transcription, cellular metabolism, DNA damage response, and aging (15–20). Besides acetylation, succinylation is another well-studied lysine PTM, which was reported to regulate the tricarboxylic acid (TCA) cycle, protein translation, and energy metabolism (21, 22). Both acetylation and succinylation use the abundant cellular metabolites, that is, acetyl-CoA and succinyl-CoA, respectively, as their acylation donors, and can occur nonenzymatically in some circumstances *in vivo* (23, 24) (Fig. 1*A*). Also, a small high-energy compound, acetyl phosphate, was reported as the donor for nonenzymatic acetylation in *E. coli* (10). Previous studies suggested that acetylation and

From the [1]Key Laboratory of Synthetic Biology, CAS Center for Excellence in Molecular Plant Sciences, Chinese Academy of Sciences, Shanghai, China; [2]CAS Key Laboratory of Quantitative Engineering Biology, Guangdong Provincial Key Laboratory of Synthetic Genomics and Shenzhen Key Laboratory of Synthetic Genomics, Shenzhen Institute of Synthetic Biology, Shenzhen Institutes of Advanced Technology, Chinese Academy of Sciences, Shenzhen, China; [3]Key Laboratory of Synthetic Biology, University of Chinese Academy of Sciences, Beijing, China; [4]Department of Cardiology, Zhongshan Hospital, Fudan University, Shanghai Institute of Cardiovascular Diseases, Shanghai, China
[‡]These authors contributed equally to this work.
*For correspondence: Wei Zhao, wei.zhao1@siat.ac.cn; Guo-ping Zhao, gpzhao@sibs.ac.cn; Peng Li, lipeng4754@163.com.
Present address for Hong Zhang: Department of Cell Biology and Molecular Genetics, University of Maryland, College Park, MD, USA.

https://doi.org/10.1016/j.mcpro.2021.100148

succinylation targeted different lysine residues and showed a preference for different residues surrounding the modified lysine sites (25). However, stochastic modifications on the same lysine residue were also observed, which were probably because of the nonenzymatic reactions (26). The combined analyses of cellular acetylome and succinylome have been reported in rice, *Pseudomonas aeruginosa*, and *Vibrio parahemolyticus* (27–29). Nevertheless, the understanding of acylation coordination remains at an early stage both *in vivo* and *in vitro*.

Because of the lack of identification of specific sirtuins, the understanding of acylations and their coordination has long been elusive in microorganisms. Our recent work in *Streptomyces coelicolor* identified an evolutionary divergent desuccinylase (*Sc*CobB2), which was different from the known deacetylase, providing a suitable model to study the crosstalk between acetylation and succinylation in bacteria (22). The desuccinylase *Sc*CobB2 regulates protein biosynthesis and carbon metabolism in *S. coelicolor* (22). The other sirtuin *Sc*CobB1 was identified as a deacetylase previously (30) and was shown to modulate the activity of chromosome segregation protein ParB (15). Here, we presented the profile of the lysine acetylome in *S. coelicolor* by combining the methods of immunoaffinity enrichment and high-accuracy MS. A large portion of the acetylated proteins was also found to be succinylated in metabolic pathways such as the TCA cycle and protein translation. The interplay between lysine acetylation and succinylation was globally explored and quantified *in vivo* and further tested by treatments with *Sc*CobB1 and *Sc*CobB2 *in vitro*. The results enriched our understanding of acylation regulation in bacteria and provided new insights into acylation coordination in cell metabolism.

EXPERIMENTAL PROCEDURES

Bacterial Strains, Media, and Materials

The wildtype *S. coelicolor* M145 was cultured in tryptic soy broth (TSB) liquid medium (50 mM glucose plus) or on MS solid medium at 30 °C. *E. coli* BL21 (DE3) was used as the host strain to express the proteins. The pan anti–acetyl-lysine and pan anti–succinyl-lysine antibodies used in this study were obtained from Jingjie PTM Biolab (Hangzhou) Co Ltd. The unmodified, acetylated, and succinylated peptides (listed in supplemental Table S1) were synthesized in Guoping Pharmaceutical (Hefei), with >98% purity.

Experimental Design and Statistical Rationale

To determine the acetylome of *S. coelicolor*, the wildtype *S. coelicolor* sample with three biological replicates and two technical replicates was prepared and analyzed using Q Exactive HF-X (Thermo Fisher Scientific). To determine the quantitative acetylome and succinylome, three samples (wildtype, Δ*SccobB1*, and Δ*SccobB2*) with three biological replicates were prepared and analyzed using label-free MS. Similar procedures were followed for the cell culture, sample preparation, peptide affinity enrichment, and LC–MS/MS analysis. The modified sites were quantified using paired *t* tests where $p < 0.05$ were considered significant. The Gene Ontology (GO)/Kyoto Encyclopedia of Genes and Genomes (KEGG) pathway/domains that presented a corrected $p < 0.05$ were considered significant.

The Determination of Cellular Acetylation and Succinylation Levels in S. coelicolor

The *S. coelicolor* wildtype cells were harvested with the interval of 1 day during the 6-day cultivation, and the whole cell proteins were then extracted. Approximately 15 μg of protein samples were separated using 12% SDS-PAGE and visualized *via* Coomassie brilliant blue staining. For the Western blotting assay, similar amounts of proteins were transferred onto the nitrocellulose membranes, and standard procedures were followed for the detection of acetylation levels. Briefly, 100 mM Tris–HCl (pH 7.5) with 0.5% (v/v) Tween-20 and 1% peptone was used for blocking, and 100 mM Tris–HCl (pH 7.5) with 0.05% (v/v) Tween-20 and 0.1% peptone was used as the primary and secondary antibody buffer. The membranes were incubated overnight with pan anti–acetyl-lysine antibody at a dilution of 1:1000 in the primary antibody buffer at 4 °C. Nitrocellulose membranes were then treated with an ECL Chemiluminescent Substrate reagent and visualized using an ImageQuant LAS 4000 mini (GE Healthcare).

Similar procedures were followed for the detection of acetylation and succinylation levels in wildtype *S. coelicolor* and its derivatives Δ*SccobB1* and Δ*SccobB2*. The pan anti–succinyl-lysine antibody with 1:2000 dilution in the primary antibody buffer was used in these studies.

Protein Extraction and Trypsin Digestion for Acylome Analysis

The wildtype *S. coelicolor* M145 and its derivatives Δ*SccobB1* and Δ*SccobB2* were cultured on MS solid medium at 30 °C for 3 days. Fresh spores were collected with a cotton swab and transferred to TSB liquid medium supplemented with 50 mM glucose. After growing for 60 h, the cells were transferred (10%) to the new TSB medium containing 50 mM glucose and harvested at the log phase after 2 days. The collected cells were first frozen and grinded into powder using liquid nitrogen and then transferred to 50-ml centrifuge tubes for sonication in lysis buffer (8 M urea, 2 mM EDTA, 5 mM DTT, 1% Protease Inhibitor Cocktail III, 3 μM trichostatin A, and 50 mM nicotinamide). Cell debris was removed by centrifugation at 12,000*g* at 4 °C for 10 min. Finally, the protein was precipitated using cold 15% trichloroacetic acid for 2 h at −20 °C. After centrifugation at 4 °C for 10 min, the supernatant was discarded. The remaining precipitate was washed with cold acetone thrice. The protein was dissolved in a buffer (8 M urea, 100 mM TEAB, and pH 8.0), and the protein concentration was determined using a 2-D Quant kit (GE Healthcare) according to the manufacturer's instructions.

For digestion, trichloroacetic acid was added slowly to make a final concentration of 20% and then the mixture was eddy mixed and precipitated at 4 °C for 2 h. The supernatant was discarded after centrifugation at 4500*g* for 5 min. The precipitate was then washed with precooled acetone 2 to 3 times. After the precipitate was dried, TEAB, with a final concentration of 200 mM, was added. The precipitate was dispersed by ultrasonication, and trypsin was added at a mass ratio of 1:50 (trypsin to protein) overnight. Then, the peptide solution was reduced with 5 mM DTT for 30 min at 37 °C and alkylated with 11 mM iodoacetamide for 15 min at room temperature in the dark.

Affinity Enrichment of Acylated Peptides

To enrich K^{ac} or K^{suc} peptides, tryptic peptides dissolved in immunoprecipitation buffer (50 mM Tris–HCl, 100 mM NaCl, 1 mM EDTA, and 0.5% NP-40; pH 8.0) were incubated with prewashed acetylation and succinylation antibody beads (PTM Biolabs) at 4 °C overnight with gentle shaking, respectively. The beads were washed four times with immunoprecipitation buffer and twice with

double-distilled water. The bound peptides were eluted from the beads using 0.1% trifluoroacetic acid. The eluted fractions were vacuum dried, and the resulting peptides were desalted using C18 ZipTips (Millipore) according to the manufacturer's instructions, followed by LC–MS/MS analysis.

LC–MS/MS Analysis

The peptides were dissolved in mobile phase A of LC and separated using the EASY-nLC 1200 UPLC system. Mobile phase A was an aqueous solution containing 0.1% formic acid and 2% acetonitrile. Mobile phase B was an aqueous solution containing 0.1% formic acid and 90% acetonitrile. Liquid phase gradient settings were 0 to 36 min, 9 to 25% B; 36 to 54 min, 25 to 35% B; 54 to 57 min, 35 to 80% B; and 57 to 60 min, 80% B. The flow rate was maintained at 500 nl/min. The resulting peptides were analyzed using a Q Exactive HF-X hybrid quadrupole-Orbitrap mass spectrometer (Thermo Fisher Scientific).

The peptides were subjected to a nanospray ionization source followed by MS/MS in Q Exactive HF-X coupled online with the UPLC. Intact peptides were detected using the Orbitrap at a resolution of 120,000. Peptides were selected for MS/MS using normalized collision energy setting 28, and ion fragments were detected in the Orbitrap at a resolution of 17,500. A data-dependent procedure that alternated between one MS scan followed by 20 MS/MS scans was applied for the top 20 precursor ions above a threshold ion count of 5E4 in the MS survey scan with a 15-s dynamic exclusion. The electrospray voltage applied was 2.1 kV. Automatic gain control was used to prevent overfilling of the ion trap, and 1E5 ions were accumulated to generate MS/MS spectra. For MS scans, the *m/z* scan range was 350 to 1600. The fixed first mass was set as 100 *m/z*.

Data Processing and Database Searches

The peak list was generated using Xcalibur 4.2.47 (Thermo Fisher). The resulting data were processed using MaxQuant (version 1.6.15.0, Max Planck Institute of Biochemistry) with the integrated Andromeda search engine. Tandem mass spectra were searched against a local UniProt *S. coelicolor* database concatenated with a reverse decoy database (Blast_Streptomyces_coelicolor_strain_ATCC_BAA-471_100226_PR_20201113.fasta; release date, November 13, 2020; 8038 sequences). Trypsin/P was specified as the cleavage enzyme allowing up to four missing cleavages, five modifications per peptide, and five charges. The mass error tolerance was set to 20 ppm for the first search, 4.5 ppm for the main search, and 20 ppm for fragment ions. Carbamidomethylation on Cys was specified as a fixed modification, and oxidation on Met, acetylation on Lys, and acetylation on protein N termini were specified as variable modifications. The false discovery rate thresholds for protein, peptide, and modification sites were specified at 1%. The minimum peptide length was set at 7. All other parameters in MaxQuant were set to default values. The site localization probability was set as >0.75.

Bioinformatics Analysis

Functional Enrichment Analysis—The GO derived from the UniProt-GOA database (http://www.ebi.ac.uk/GOA/) was used to annotate the functions of proteins in the acetylome. The database of KEGG was used to annotate the pathways. To identify the enriched GO/KEGG pathways, the Functional Annotation Tool of DAVID Bioinformatics Resources (31) and InterPro database (32) were used against the background of *S. coelicolor* proteome. A two-tailed Fisher's exact test was employed to test the protein enrichments.

Motif Analysis for Lysine Acetylation Substrates—Programs Motif-X (Harvard Medicine School) (33) and iceLogo (Universiteit Gent) (34) were used to analyze the model of identified acetylation sequences of acetyl-21-mers (10 amino acids upstream and downstream of the acetylation site). The *S. coelicolor* proteome sequences were used as the background database parameter, and other parameters were set to default values. In addition, an in-house R-package script (35) was used to generate the position-specific heat map by plotting the $\log_{10}$ ratio values of frequencies.

Protein–Protein Interaction Network—The acetylated proteins were searched against the STRING database version 9.1 (36) for protein–protein interactions. Only interactions between proteins belonging to the searched dataset were selected. The interaction network from STRING was visualized using Cytoscape (National Resource for Network Biology) (37). A graph obtained from the clustering algorithm, molecular complex detection (MCODE) (38), was utilized to analyze densely connected regions. MCODE is a plug-in in the network analysis kit, and the graph was visualized using Cytoscape.

*Cloning, Expression, and Purification of Sc*CobB1, Sc*CobB2, and CobBL*—The plasmids pET28b-*Sc*CobB1/*Sc*CobB2/CobBL were constructed using a previously reported method (22). The correct plasmids were checked using PCR and then transformed into BL21. A single colony was picked and transferred into a 5-ml LB medium containing kanamycin overnight and then 1:100 diluted into a 500-ml LB liquid medium at 37 °C. When the absorbance at 600 nm reached about 0.6, the cells were transferred to 16 °C and induced with 0.5 mM IPTG overnight.

The cells were harvested by centrifugation at 6000 rpm for 10 min at 4 °C and then suspended in a buffer containing 25 mM Tris–HCl (pH 8.0), 150 mM NaCl, 1 mM DTT, 10% (v/v) glycerol, and 25 mM imidazole. After lysis with the cell disruptor, cellular debris was removed by centrifugation at 13,000*g* for 30 min at 4 °C. The collected supernatants were loaded onto a 5-ml nickel resin column (GE Healthcare). After washing with 10 volumes of wash buffer (25 mM Tris–HCl, 150 mM NaCl, and 20 mM imidazole; pH 8.0), the proteins were eluted (elution buffer, 25 mM Tris–HCl, 150 mM NaCl, and 500 mM imidazole; pH 8.0). The proteins were subjected to the AKTA purification system (GE Healthcare), quantified, aliquoted, and stored at –80 °C.

Quantification of Peptide Deacetylation and Desuccinylation Using HPLC—The *in vitro* peptide deacylation system contained 50 mM Tris buffer (pH 8.0), 50 mM NaCl, 1.0 mM DTT, 6.0 mM $MgCl_2$, 10.8 μM *Sc*CobB1 or 3.6 μM *Sc*CobB2/CobBL, 1.0 mM NAD^+, and 540 μM acylated peptide. The reactions were carried out at 30 °C overnight in a 50-μl volume, and quenched with 1 volume of 10% (v/v) trifluoroacetic acid for 10 min at room temperature. The mixture was centrifuged at 13,000*g* for 10 min to discard the sediment, and the supernatant was subjected to HPLC (Agilent Technologies) using the Aeris peptide XB-C18 column (150 × 4.6 mm, 3.6 μm; Phenomenex). The mobile phase consisted of solvent A (0.1% formic acid in HPLC-grade water) and solvent B (HPLC-grade acetonitrile). Peptides were eluted in a linear gradient of 5 to 100% solvent B at a rate of 1 ml min^{-1} over 30 min. The column temperature was set at 25 °C, and the peptides were monitored by UV light at a wavelength of 215 nm. The deacylation activities of *Sc*CobB1, *Sc*CobB2, and CobBL were determined by calculating the peak area of the peptides as follows:

$$\text{Deacylation percentage} = \frac{\text{Deacylation}}{\text{Deacylation} + \text{acylation}}$$

RESULTS

Detection of Abundant and Dynamic Acetylation in S. coelicolor

The representative *Streptomyces* are a group of soil-dwelling microorganisms notable for their complex lifecycles and antibiotic production capacity (39). Our recent work in

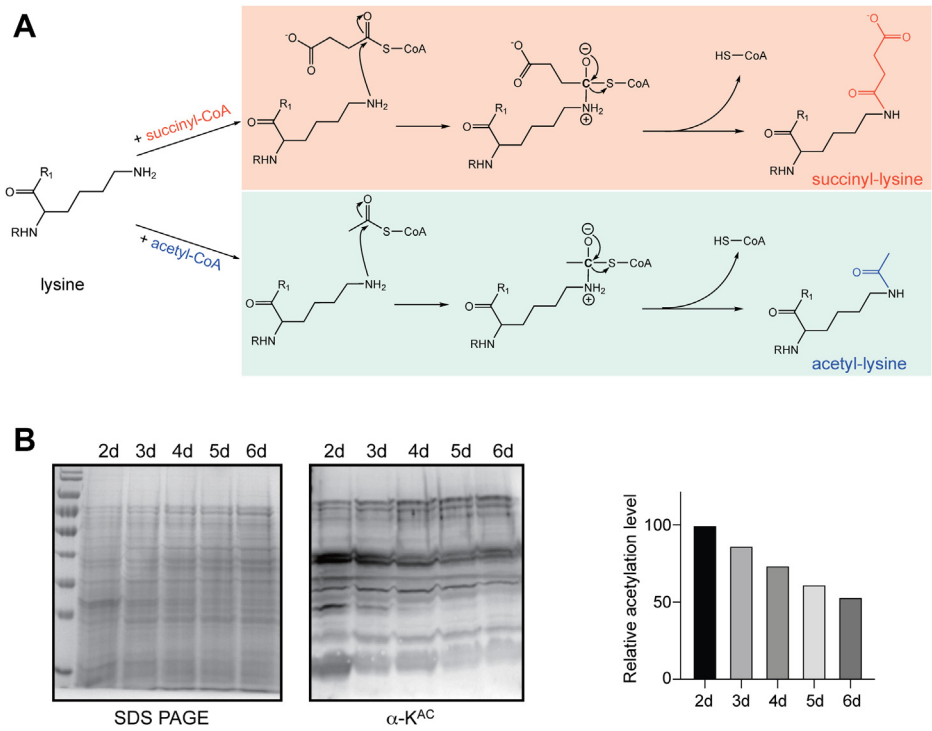

FIG. 1. **Highly abundant and dynamic acetylation in *Streptomyces coelicolor*.** *A*, lysine acetylation by acetyl-CoA and lysine succinylation by succinyl-CoA are shown in detail. *B*, the acetylation level in *S. coelicolor* was determined using Western blotting, displaying highly abundant and dynamic modification in cells. Cell lysates were separated by 12% SDS-PAGE, and the pan anti–acetyl-lysine antibody was used (*left panel*). The relative acetylation levels were normalized to the loading protein levels and quantified with ImageJ (*right panel*). The normalized value from the first line of the gel (sample of the second day) was set as 100%.

S. coelicolor discovered highly abundant and dynamic acetylation (Fig. 1*B*). The intensities of cellular acetylation signals varied from the culture time. Moreover, a full range of signal decrease along the cell growth was observed, suggesting possible global regulation of acetylation in *S. coelicolor.*

Acetylome Analyses in S. coelicolor

To acquire detailed information on acetylation regulation in *S. coelicolor*, acetylome analyses were performed by culturing the cells in TSB medium containing 50 mM glucose. The cells were harvested at the midlog phase, and the proteins were extracted for trypsin digestion. The acetylated peptides were then enriched by affinity purification using pan acetyl-lysine antibody and subjected to LC–MS/MS analysis with a high accuracy mass spectrometer. An overview of the experimental procedures is shown in Figure 2*A*. A total of 1298 lysine acetylation sites in 601 proteins were identified using the UniProt database. Detailed information for all the acetylated peptides and their matched proteins is provided in supplemental Table S2. We checked the quality of our MS data and inspected the distribution of mass errors for all the identified peptides. As presented in supplemental Figure S1, all the results suggested that the MS data met the requirements for the acetylome analysis (40).

To better understand the lysine acetylated proteins in *S. coelicolor*, we performed functional annotation analysis using GO. The results showed that the acetylated proteins are widely located in *S. coelicolor* cells and participated in a variety of biological processes (supplemental Fig. S2 and supplemental Table S3). The classification based on biological processes showed that most acetylated proteins were involved in cell metabolism (36.5%) and cellular processes (27.2%). The classification based on molecular function showed that most acetylated proteins possessed the catalytic (47%) or DNA-binding (39.6%) activities. A high amount of acetylated proteins were located in the cell cytoplasm in comparison to other cellular components, consistent with previous reports (4, 41).

The GO enrichment analysis for the acetylated proteins showed that acetylation substrates were mostly enriched in protein biosynthesis, and the top two acetylated biological processes were protein translation and metabolism (Fig. 2*B* and supplemental Table S4). The function of lysine acetylated substrates included structural constituents of ribosome and RNA binding (Fig. 2*C*). The functional enrichment analyses were performed using the KEGG database as well. The acetylated proteins were found to be enriched in protein biosynthesis in addition to other metabolic pathways. The top three enriched KEGG pathways were ribosome biogenesis, TCA cycle, and aminoacyl-tRNA biosynthesis (Fig. 2*D* and

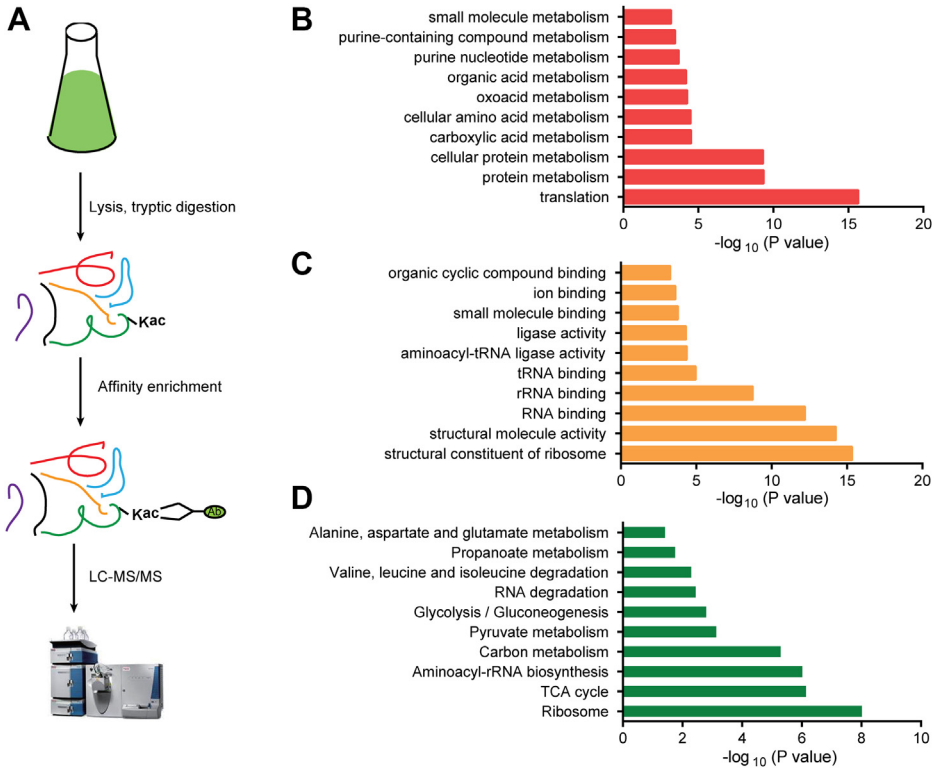

FIG. 2. **The acetylome analysis highlights the acetylation regulation in protein translation and metabolism in *Streptomyces coelicolor*.** *A*, schematic representation of the workflow used in profiling of acetyl proteomics in *S. coelicolor*. Gene Ontology (GO) enrichment analysis for acetylome based on biological processes (*B*) and molecular function analyses (*C*). Kyoto Encyclopedia of Genes and Genomes (KEGG) pathway enrichment analysis revealed that acetylation proteins were enriched in protein translation and metabolism pathways (*D*).

supplemental Table S5). Taken together, both GO annotation and KEGG pathway analyses suggested that the substrates related to protein translation and metabolism were extensively regulated by acetylation in *S. coelicolor*.

Functional Interaction Networks of Acetylated Substrates in S. coelicolor

Protein–protein interactions occur widely in all organisms and are important in implementing and regulating cellular processes. However, how the acetylated protein interactions affect the regulation of *S. coelicolor* physiology and development is poorly understood. The interaction network of acetylated proteins was generated based on the STRING database and visualized using Cytoscape (36). A total of 462 acetylated proteins were identified as nodes and connected to each other (Fig. 3*A* and supplemental Table S6). Functional category analysis for these proteins demonstrated several highly interconnected clusters such as ribosome biogenesis, carbon metabolism, protein folding, and aminoacyl-tRNA biosynthesis (Fig. 3). Consistent with the GO and KEGG analysis results (Fig. 2), most acetylated proteins were enriched in protein translation and metabolic pathways in general. The top two identified clusters were ribosome-associated proteins (Fig. 3*B*) and carbon metabolism (Fig. 3*C*). The strong interactions among these acetylated pathway components suggested that acetylation may facilitate *S. coelicolor* to adapt to the changing soil environments.

Sequence Motifs of Acetylation in S. coelicolor

The preferences for the amino acid motifs surrounding acetylation sites were observed in both prokaryotes and eukaryotes (4, 42–44). Here, the Motif-X program was used to search for overrepresented sequence patterns among all identified acetylated peptides. The preferred conserved consensus motifs with amino acid sequences from the −10 to +10 flanking region of the acetylated lysine were extracted (supplemental Table S7). As shown in Figure 4*A*, eight conserved sequences surrounding K^{ac} sites were detected in the *S. coelicolor* acetylome. These motifs included ##K^{ac}#F##, ##I#K^{ac}##, ##K^{ac}#H##, ##K^{ac}H##, ##FK^{ac}##, ##V#K^{ac}##, ##K^{ac}L##, and ##LK^{ac}## (# indicates a random amino acid residue). The amino acids F, H, and L were frequently found in these motifs. Among the acetylation motifs identified here, motifs ##I#K^{ac}##, ##K^{ac}#F##, ##K^{ac}#H##, ##K^{ac}H##, ##FK^{ac}##, and ##V#K^{ac}## were mainly present as substrates

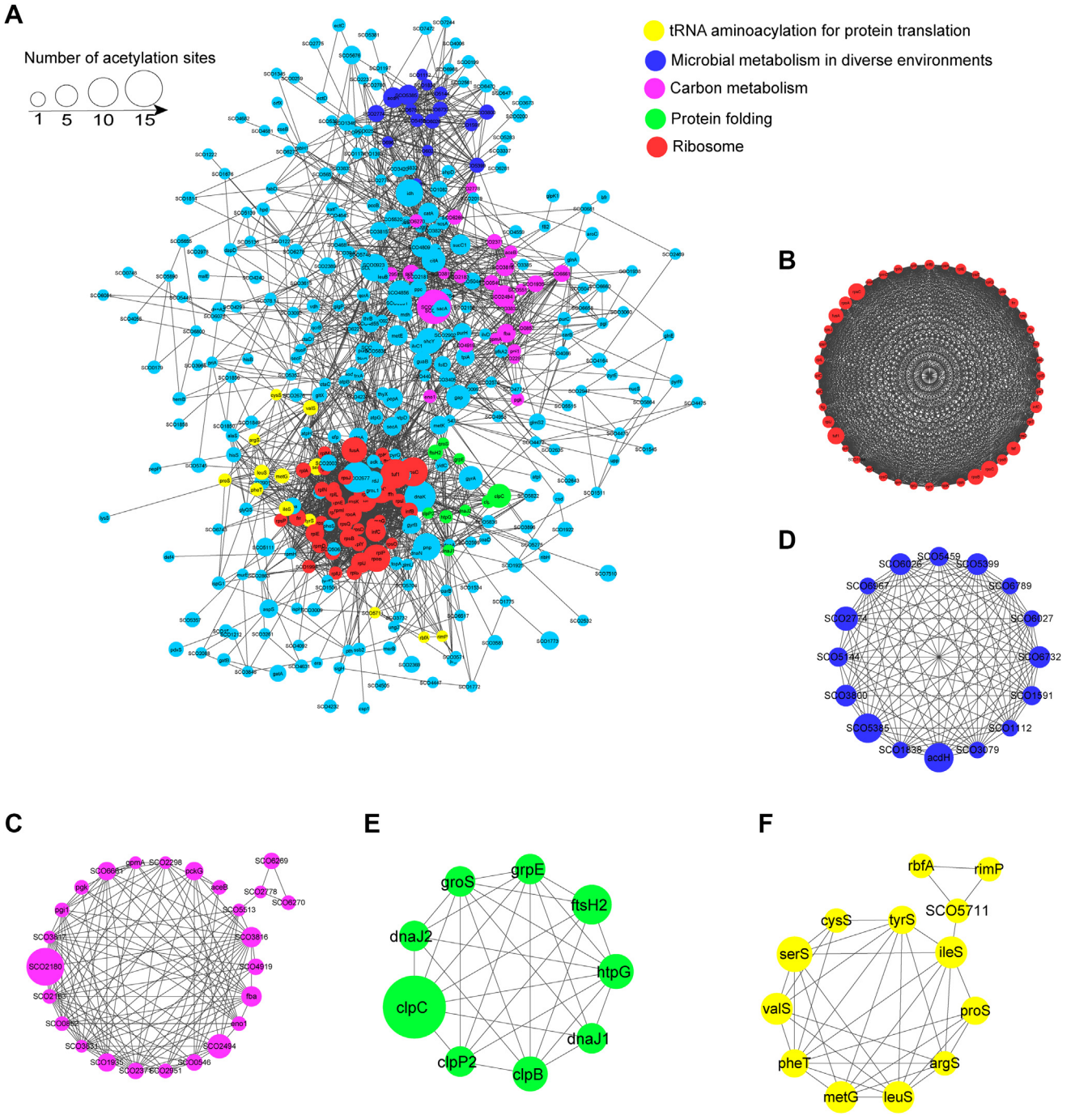

FIG. 3. **Protein–protein interaction networks of acetylated proteins in *Streptomyces coelicolor*.** Interaction networks of acetylated proteins were analyzed using the MCODE plug-in toolkit in the Cytoscape software. *A*, interaction network of all acetylated proteins. Detailed cluster information of proteins in ribosomes (*B*), carbon metabolism (*C*), metabolism in diverse environments (*D*), protein folding (*E*), and tRNA aminoacylation in translation (*F*) is shown. The respective MCODE score and protein–protein interaction score were listed in supplemental Table S6.

in fungi (45), and the motifs ##K^{ac}H##, ##FK^{ac}##, and ##LK^{ac}## have also been reported as representatives in rice (44) and bacteria (46, 47). These results supported the notion that the preferred sequences for lysine acetylation are conserved among different organisms, implying a similar kinetics of acetylation.

The other two software, iceLogo and R program, were also used to analyze the acetylation motifs, and similar results were obtained. The heat map produced using the R program analysis not only showed the same over-represented flanking sequences as in Motif-X program but also displayed that arginine (R) and lysine (K) tend to be

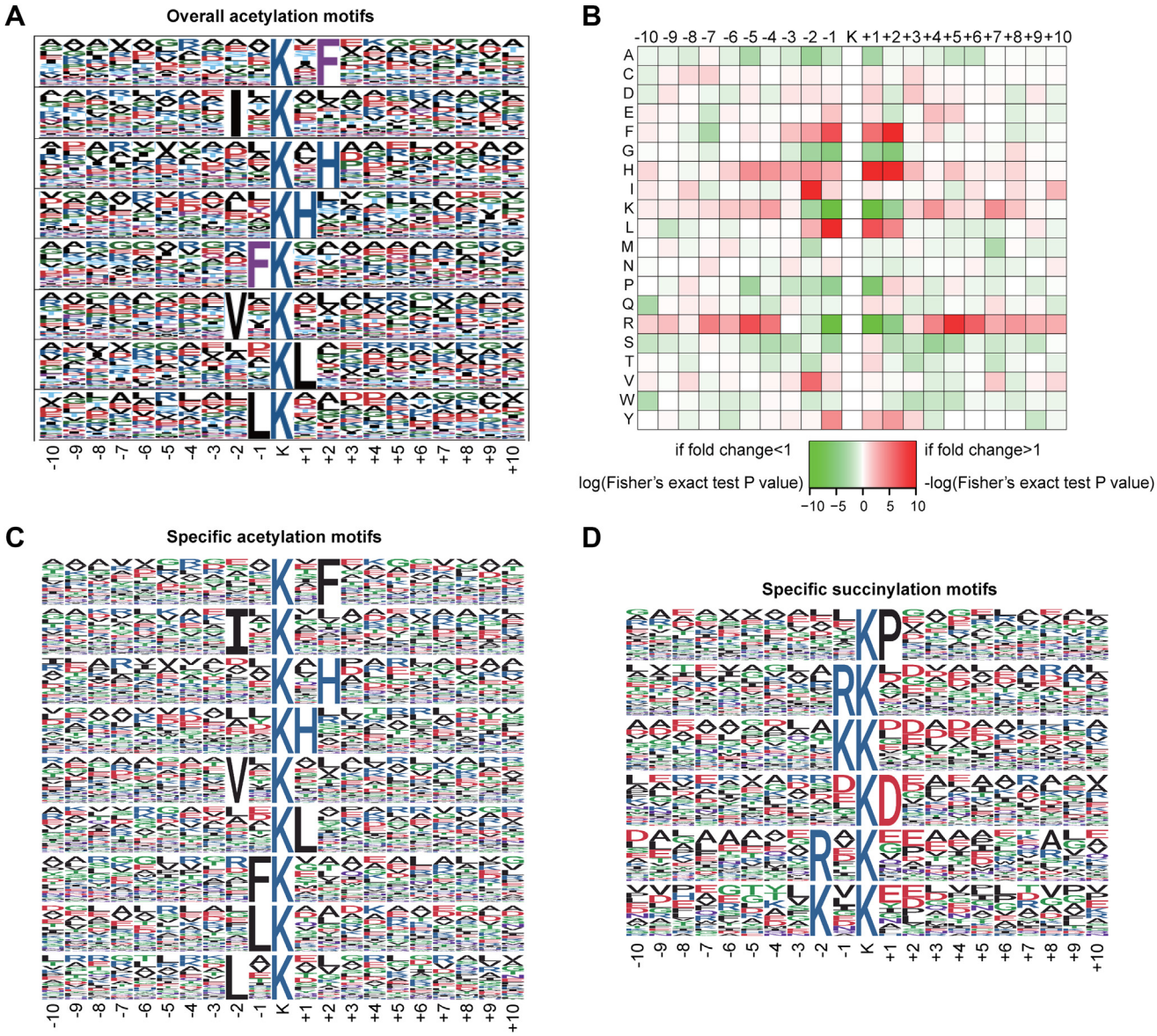

FIG. 4. **Analysis of acylation motifs in *Streptomyces coelicolor*.** *A*, sequence logo representation of overall acetylation motifs identified using Motif-X software. The motifs consisted of 20 residues (ten amino acids upstream and the other ten downstream to the site) surrounding the acetylated lysine. *B*, the under-represented and over-represented amino acids flanking the acetylated sites were shown using a heat map generated from the R-package script. *C*, the specific acetylation motifs by comparing acetylome and succinylome data. *D*, the specific succinylation motifs by comparing acetylome and succinylome data. The representatives of these motifs were analyzed by Motif-X.

absent at the −1 and +1 positions around K^{ac}, suggesting that they are unpopular residues in the substrate sequences near K^{ac} (Fig. 4*B*). iceLogo displayed similar results as the other software for both overrepresented and underrepresented flanking sequences of the acetylated lysine residues (supplemental Fig. S3).

The acetylation motifs showed completely different patterns compared with those of succinylation (Fig. 4). Particularly, the acetylation motifs displayed opposite preferences for the residues arginine (R) and lysine (K), which were the representatives in succinylation motifs near K^{suc} (22). The specific and overlapped patterns of the modified motifs were then analyzed. As shown in Figure 4, *C* and *D*, the specific motifs mimicked the full modification spectrums in acetylation and succinylation, respectively. Also, no obvious overlapped motifs were identified between acetylation and succinylation, indicating that bimodification on the same lysine residue was likely from the stochastic events and with no specificity. Collectively, these results supported the notion that acetylation and succinylation target different lysine residues in the proteome, and moreover, stochastic bimodifications on some lysine residues were also inferred.

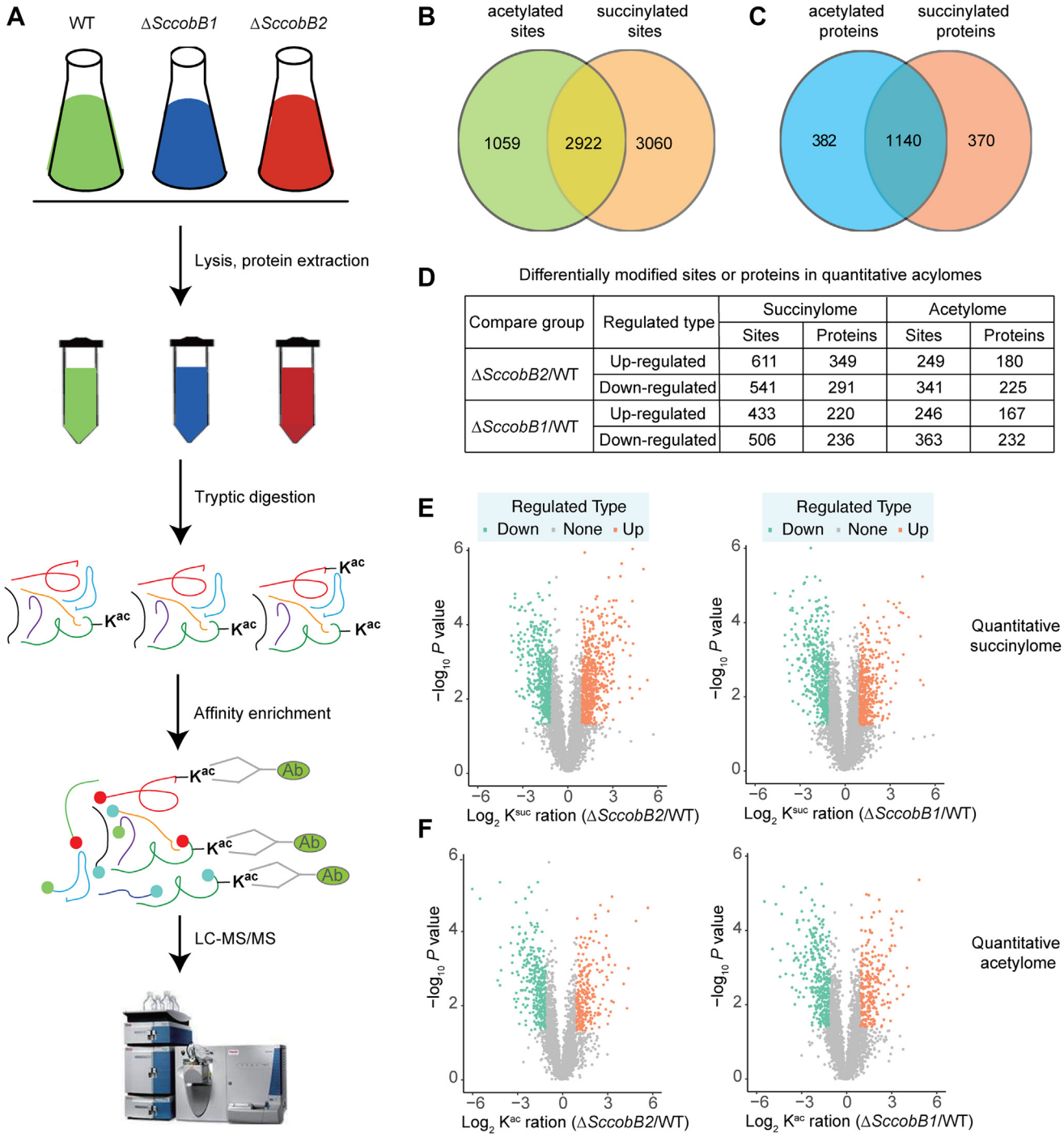

Compare group	Regulated type	Succinylome		Acetylome	
		Sites	Proteins	Sites	Proteins
ΔSccobB2/WT	Up-regulated	611	349	249	180
	Down-regulated	541	291	341	225
ΔSccobB1/WT	Up-regulated	433	220	246	167
	Down-regulated	506	236	363	232

FIG. 5. **Quantitative acylome analyses after knocking out *SccobB1* or *SccobB2*.** *A*, schematic representation of the workflow used in quantitative acylome analyses. The quantitative acetylome and quantitative succinylome analyses were performed following the similar procedures (see Experimental Procedures section). Only the quantitative acetylome was shown here to simplify. *B*, the intersection of acetylated and succinylated sites in *Streptomyces coelicolor* proteomes. *C*, the intersection of acetylated and succinylated proteins in *S. coelicolor* proteomes (the bimodified proteins including those with acetylation and succinylation at separate sites in one protein). *D*, the summary number of the differentially modified sites or proteins in quantitative acylomes. *E*, scatter plot showed the details of changes in succinylated peptide intensities between the *S. coelicolor* wildtype and Δ*SccobB2* cells (*left*) and between the wildtype and Δ*SccobB1* cells (*right*). *F*, scatter plot showed the details of changes in acetylated peptide intensities between the *S. coelicolor* wildtype and Δ*SccobB2* cells (*left*) and between the wildtype and Δ*SccobB1* cells (*right*). When $p < 0.05$, the change of modification level >2 was deemed as upregulated significantly (*brown dots*), and the change modification level <0.5 was deemed as downregulated significantly (*cyan dots*).

The Crosstalk Between Acetylation and Succinylation in S. coelicolor

A previous study has shown that pathways involved in protein biosynthesis and carbon metabolism were enriched by succinylation in *S. coelicolor* (22). In the current study, the identified acetylation substrates were also closely related to protein translation and central metabolic processes (Figs. 3 and 4). Key questions are raised that whether there is any crosstalk between lysine acetylation and succinylation and, if so, how it is regulated by the different sirtuins. To address these questions, quantitative acetylome and succinylome analyses were performed by knocking out either the desuccinylase *Sc*CobB2 or the presumed deacetylase *Sc*CobB1 (30) (Fig. 5*A*). The bacterial cells were cultured and harvested using the same conditions as shown in Figure 2*A*. In total, 3981 sites in 1522 proteins and 5982 sites in 1510 proteins were quantified in acetylome and succinylome, respectively (supplemental Table S8). The combined results revealed that 2511 sites were both acetylated and succinylated, accounting for 63.1% and 50.0% of the identified sites in acetylome and succinylome, respectively (Fig. 5*B* and supplemental Table S9). The bimodified proteins (1140) including those with acetylation and succinylation at the same sites and different sites in one protein, accounts for 74.9% and 75.5% of all the identified acetylome and succinylome proteins, respectively, suggesting extensive crosstalk between lysine acetylation and succinylation in *S. coelicolor* (Fig. 5*C* and supplemental Table S9).

After deletion of *SccobB2*, the quantitative analyses showed that more sites (611 *versus* 541) were upregulated in succinylation, consistent with the previous notion that *Sc*CobB2 is a global desuccinylase (22) (Fig. 5, *D* and *E*). On the other hand, when *SccobB1* was deleted, more sites (506 *versus* 433) were downregulated in succinylation (Fig. 5, *D* and *E*), indicating that some lysine sites modified by succinylation might also be targeted by *Sc*CobB1. As we know, no desuccinylase but a deacetylase activity was reported for *Sc*CobB1 previously (30). The quantitative acetylome results showed that more sites (341 *versus* 249) were downregulated in acetylation after deletion of *SccobB2* (Fig. 5, *D* and *F*), suggesting some lysine sites modified by acetylation could also be targeted by *Sc*CobB2. However, less upregulated acetylation sites (246 *versus* 363) were observed in Δ*SccobB1* (Fig. 5, *D* and *F*). This result implied other deacetylase(s) besides *Sc*CobB1 may exist and play a leading role in *S. coelicolor*. Nevertheless, these observations from the quantitative analyses revealed a possible competitive relationship between acetylation and succinylation targeting upon the same lysine sites.

To investigate the functional categories of the differentially modified proteins, Clusters of Orthologous Groups analysis was performed for the upregulated and downregulated proteins in both the quantitative acetylome and succinylome (supplemental Fig. S4). The quantitative succinylome results showed that the most upregulated proteins in Δ*SccobB2* were involved in gene transcription and protein translation, whereas the most downregulated proteins in Δ*SccobB1* were involved in cell metabolism. These results indicated that distinct proteins were regulated by *Sc*CobB1 and *Sc*CobB2, in agreement with the results of the motifs analysis shown in Figure 4. The quantitative acetylome results (supplemental Fig. S4) showed that the most downregulated proteins were involved in cell metabolism and signal transduction both in Δ*SccobB1* and Δ*SccobB2*, implying *Sc*CobB1 may not be the primary deacetylase and a coordination of *Sc*CobB1 and *Sc*CobB2 in the regulation of *S. coelicolor* acetylation to some extent.

To better understand the role of the PTM crosstalk, we mapped the bimodified proteins onto the KEGG pathways. The results showed that multiple pathways, particularly those involved in ribosome biogenesis and central metabolism, were enriched by bimodified proteins (Fig. 6 and supplemental Table S10). In detail, 42 of 53 ribosomal proteins were bimodified by acetylation or succinylation. RpoA/RpoB/RpoC, EF-Tu/EF-Ts, and FtsY/Ffh were the top ribosomal complexes whose subunits were both acetylated and succinylated (Fig. 6*A* and supplemental Fig. S5*A*). Nearly all the enzymes (85.7%) in central metabolism pathways were bimodified. Remarkably, enzymes in the TCA cycle were 100% bimodified, including α-ketoglutarate dehydrogenase components (SucAB), succinyl-CoA synthetase complexes (SucCD), and fumarate hydratase (Fig. 6*B*). In addition, all the enzymes from the glycolysis/gluconeogenesis pathway were identified as bimodified as well (Fig. 6*C*). It is worth noting that glyceraldehyde-3-phosphate dehydrogenase (GapA), which is a rate-limit enzyme in the glycolysis pathway, was extensively acetylated and succinylated (Fig. 6*C* and supplemental Fig. S5*B*). In GapA, 15 lysine sites were acetylated and 20 lysine sites were succinylated including 14 lysine sites were bimodified, and most of them were on the conserved enzymatic activity domains (5). The modified sites in response to *SccobB1* or *SccobB2* deletion were also quantified and mapped onto the KEGG pathways (Fig. 6 and supplemental Table S10), providing a bunch of candidates that were highly regulated by acetylation and succinylation. RpoA/RpoB/RpoC, GapA, AceE, SucAB, and fumarate hydratase had the most upregulated succinylation sites in Δ*SccobB2*, whereas AceE, citrate synthase, and SucA had the most upregulated acetylation sites in Δ*SccobB1* (Fig. 6). Collectively, 91.9% of the sites were identified as acetylation and succinylation in the central metabolic pathway proteins, far higher than the average level of the bimodification sites (Fig. 5*B*), implying that more nonenzymatic reactions might be occurring in these pathways. Taken together, our analyses indicated extensive crosstalk between acetylation and succinylation both on the same sites and same proteins involved in the metabolic pathways.

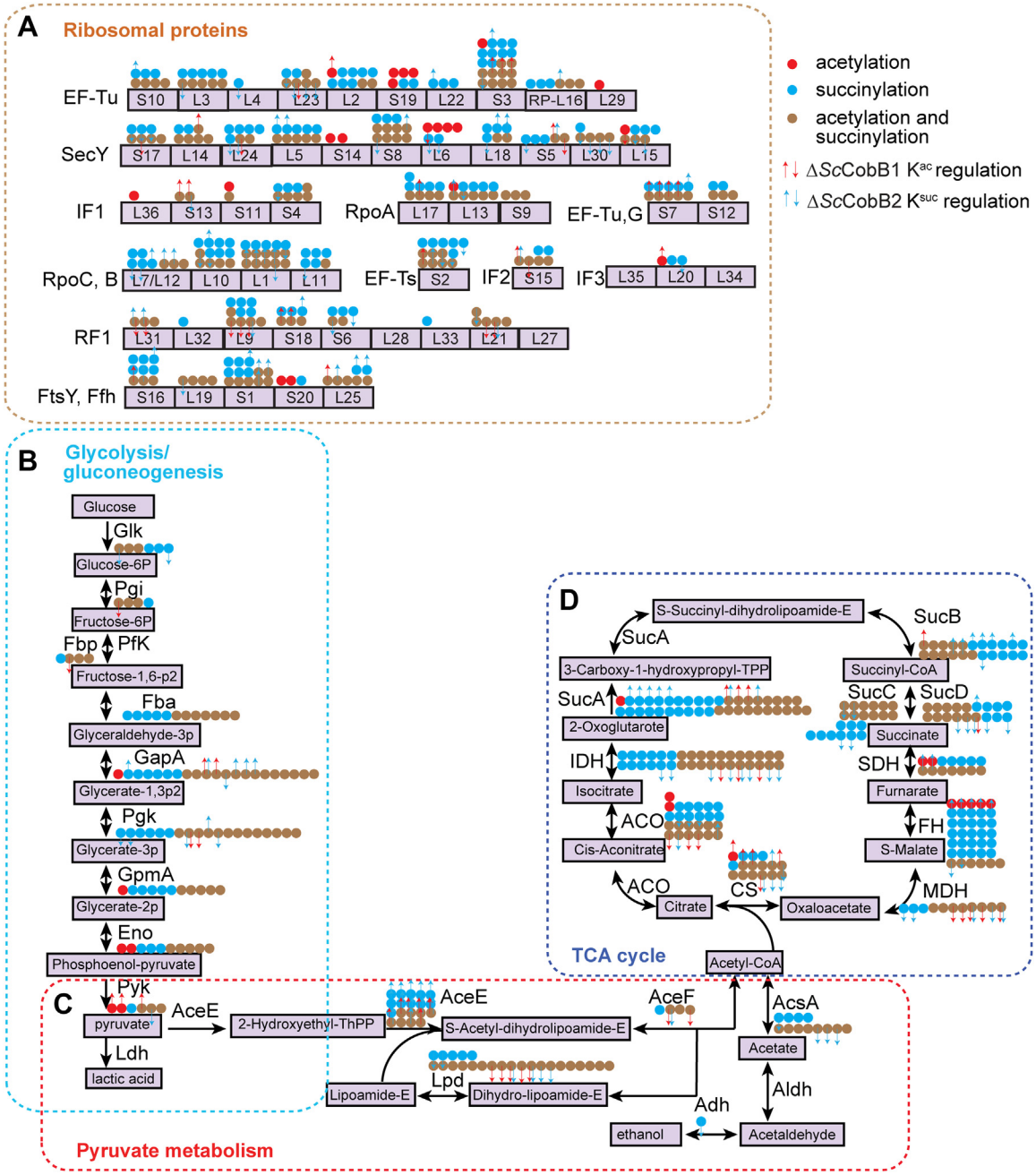

FIG. 6. **The enriched bimodified proteins are involved in protein translation and carbon metabolism pathways.** The bimodified (acetylated and succinylated) proteins enriched in ribosomes (*A*), glycolysis/gluconeogenesis (*B*), pyruvate metabolism (*C*), and tricarboxylic acid (TCA) cycle (*D*) were mapped onto the Kyoto Encyclopedia of Genes and Genomes (KEGG) pathways. The acetylation-only sites are shown as *red dots*, succinylation-only sites are shown as *blue dots*, and bimodified sites are shown as *brown dots*. The modified sites in response to knocking out of *SccobB1* or *SccobB2* were quantified and mapped onto the KEGG pathways. The acetylation sites regulated by Δ*SccobB1* and the succinylation sites regulated by Δ*SccobB2* are shown in *red and blue arrows*, respectively. ACO, aconitate hydratase; AceE, pyruvate dehydrogenase E1 component; AceF, pyruvate dehydrogenase E2 component (dihydrolipoamide acetyltransferase); AcsA, acetyl-CoA synthetase; Adh, alcohol dehydrogenase; Aldh, aldehyde dehydrogenase; CS, citrate synthase; Eno, phosphopyruvate hydratase; Fba, fructose-bisphosphate aldolase; FH, fumarate hydratase; GapA, glyceraldehyde-3-phosphate dehydrogenase; Glk, glucokinase; GpmA, phosphoglycerate mutase; IDH, isocitrate dehydrogenase; Lpd, dihydrolipoamide dehydrogenase; MDH, malate dehydrogenase; N-resize, upregulated; PfkA, 6-phosphofructokinase; Pgi, glucose-6-phosphate isomerase; Pgk, phosphoglycerate kinase; Pyk, pyruvate kinase; S-resize, downregulated; SDH, succinate dehydrogenase; SucA, 2-oxoglutarate dehydrogenase E1 component; SucB, 2-oxoglutarate dehydrogenase E2 component; SucC, acetyl-CoA synthetase subunit beta; SucD, acetyl-CoA synthetase subunit alpha.

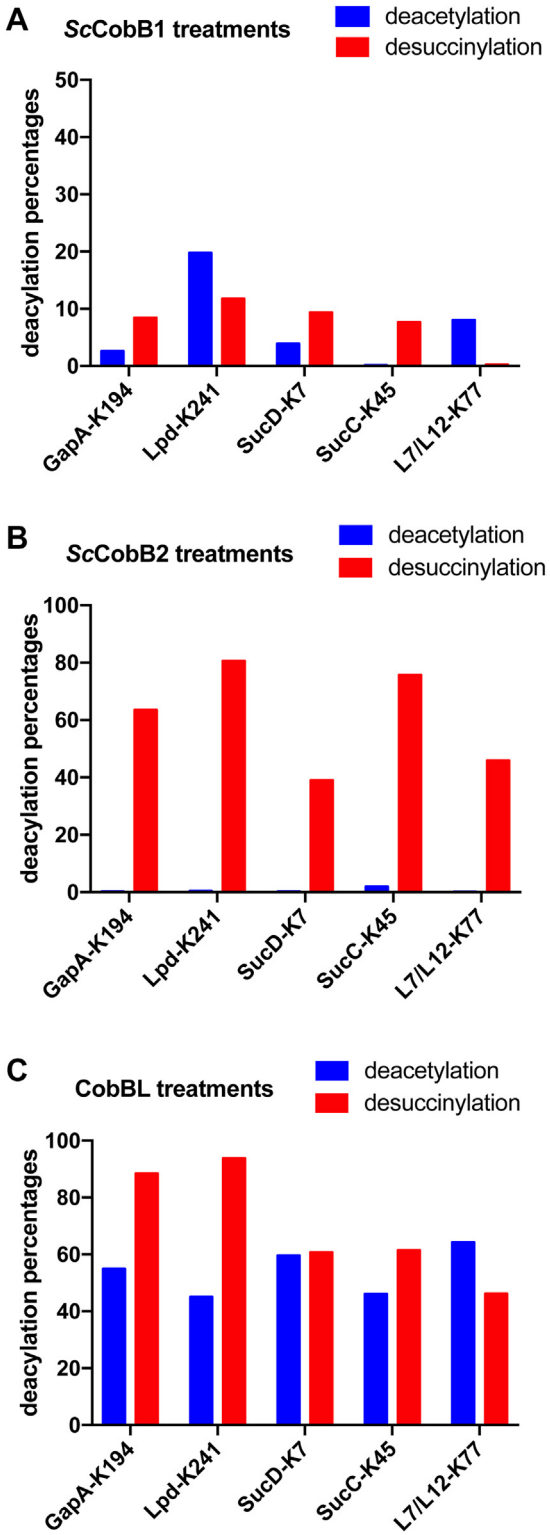

FIG. 7. **Deacylation analysis using *Sc*CobB1 and *Sc*CobB2 *in vitro*.** The regulatory crosstalk between deacetylation and desuccinylation was tested by treating the same synthetic peptides with sirtuins. The assays were performed as explained in the *Experimental procedures* section, using NAD^+ as the cofactor. The assays without NAD^+ in the mixtures were used as the negative controls (see supplemental Fig. S5 for more details). *A*, the modified peptides were incubated with *Sc*CobB1. Relatively, low deacetylase and desuccinylase activities were observed. *B*, the modified peptides were incubated with *Sc*CobB2. A specific desuccinylase activity was observed. *C*, the bifunctional CobBL was used as a positive control that showed both the deacetylase and desuccinylase activities.

Deacylation by Sirtuins In vitro

To further explore the interplay between acetylation and succinylation, *in vitro* tests were performed by treating these sites with different sirtuins. Five lysine-containing peptides were randomly selected from metabolic pathways showing both acetylation and succinylation (supplemental Table S1). These peptides and their corresponding acetylated and succinylated products were synthesized and tested with *Sc*CobB1 or *Sc*CobB2 treatment *in vitro*, using the *E. coli* CobBL treatment as the positive control. As shown in Figures 7 and S6, all the succinylated peptides were desuccinylated by *Sc*CobB2, whereas all the acetylated peptides except SucC-K45^{ac} were deacetylated by *Sc*CobB1, demonstrating evident crosstalk by different sirtuins. As expected, *Sc*CobB2 displayed a specific desuccinylase activity (Fig. 7*B*), and CobBL displayed both deacetylase and desuccinylase activities (Fig. 7*C*). However, *Sc*CobB1 was not shown as a specific deacetylase, and it also displayed weak desuccinylase activity for some peptides (Fig. 7*A*). In summary, these results confirmed the regulatory crosstalk of PTMs in *S. coelicolor*. The deacylation by *Sc*CobB1 and *Sc*CobB2 may work together in elaborately regulating cellular biological processes (*e.g.*, cell metabolism).

DISCUSSION

In the current study, we reported the first proteome-wide analysis of lysine acetylation and quantitative proteomic analyses including both acetylation and succinylation in *S. coelicolor*. Bioinformatics analysis showed that the acetylated proteins were involved in a broad range of cellular functions ranging from protein translation to cellular metabolic pathways (Fig. 2). Comparative analysis revealed that the acetylation and succinylation highly overlapped in proteins as well as in some lysine loci in *S. coelicolor* proteomes (Figs. 4–6). Also, distinct motif patterns of acetylation and succinylation were suggested in this study (Fig. 4), supporting the notion that the two PTMs targeted different lysine residues (25). The stochastic modifications on the same lysine residues might be due to the nonenzymatic reactions by either succinyl-CoA or acetyl-CoA (or acetyl phosphate) (10, 23). In addition, our *in vitro* experiments suggested possible regulatory crosstalk by sirtuins, which indicated a coordination between acetylation and succinylation to regulate *S. coelicolor* physiology. However, more analyses are still needed to uncover the physiological significance underlining the stochastic

modifications as well as the competitive relationship between the sirtuins.

In the current study, we confirmed the desuccinylase activity of *Sc*CobB2 both *in vivo* (Fig. 6) and *in vitro* (Fig. 7). However, because of the relatively weak deacetylase activity shown by *Sc*CobB1 (Figs. 5*D* and 7), we still cannot exclude the possibility that another global deacetylase(s) is functional in *S. coelicolor*. Although the mechanism for the acylation crosstalk remains unclear, our systemic analysis provided a basis for further exploration of the roles of PTMs in cell metabolism as well as other pathways in *S. coelicolor*. Future directions could include investigating the dynamic homeostasis of the acylations *in vivo* and characterizing other possible deacetylases in *S. coelicolor*.

DATA AVAILABILITY

The MS proteomics data have been deposited to the ProteomeXchange Consortium *via* the PRIDE partner repository (48) with the dataset identifier PXD027205 and PXD019536. The results were created using MaxQuant with version 1.6.15.0. Alternatively, the dataset can be accessed in MS-Viewer (49) with the search key "zbzofokood" (quantitative succinylome) and "schqt1dyvv" (quantitative acetylome).

Supplemental data—This article contains supplemental data.

Acknowledgments—We thank Jingjie PTM Biolab (Hangzhou, China) for help in analyzing the proteomic data.

Funding and additional information—This work was supported by the National Key R&D Program of China (2019YFA0904003 to W. Z.), Strategic Priority Research Program of the Chinese Academy of Sciences, China (XDB38020300 to W. Z.), National Natural Science Foundation of China (31921006 to G.-p. Z. and 82000273 to P. L.), Guangdong Basic and Applied Basic Research Foundation (2021A1515012511 to W. Z.), and China Postdoctoral Science Foundation (BX20200092 to P. L.).

Author contributions—P. L., G.-p. Z., and W. Z. methodology; H. Z., Y. Y., and J. W. formal analysis; H. Z. and Y. Y. investigation; F. L., Z. G., and S. Z. resources; W. Z. writing–original draft.

Conflict of interest—The authors declare no competing interests.

Abbreviations—The abbreviations used are: GO, Gene Ontology; KEGG, Kyoto Encyclopedia of Genes and Genomes; PTM, post-translational modification; SIRT, sirtuin; TCA, tricarboxylic acid; TSB, tryptic soy broth.

Received July 16, 2021 Published, MCPRO Papers in Press, September 14, 2021, https://doi.org/10.1016/j.mcpro.2021.100148

REFERENCES

1. Walsh, C. T., Garneau-Tsodikova, S., and Gatto, G. J., Jr. (2005) Protein posttranslational modifications: The chemistry of proteome diversifications. *Angew. Chem. Int. Ed. Engl.* **44**, 7342–7372
2. Wang, Z. A., and Cole, P. A. (2020) The chemical biology of reversible lysine post-translational modifications. *Cell Chem. Biol.* **27**, 953–969
3. Wang, Q., Zhang, Y., Yang, C., Xiong, H., Lin, Y., Yao, J., Li, H., Xie, L., Zhao, W., Yao, Y., Ning, Z. B., Zeng, R., Xiong, Y., Guan, K. L., Zhao, S., *et al*. (2010) Acetylation of metabolic enzymes coordinates carbon source utilization and metabolic flux. *Science* **327**, 1004–1007
4. Zhang, J., Sprung, R., Pei, J., Tan, X., Kim, S., Zhu, H., Liu, C. F., Grishin, N. V., and Zhao, Y. (2009) Lysine acetylation is a highly abundant and evolutionarily conserved modification in *Escherichia coli*. *Mol. Cell. Proteomics* **8**, 215–225
5. Zhang, Z., Tan, M., Xie, Z., Dai, L., Chen, Y., and Zhao, Y. (2011) Identification of lysine succinylation as a new post-translational modification. *Nat. Chem. Biol.* **7**, 58–63
6. Peng, C., Lu, Z., Xie, Z., Cheng, Z., Chen, Y., Tan, M., Luo, H., Zhang, Y., He, W., Yang, K., Zwaans, B. M., Tishkoff, D., Ho, L., Lombard, D., He, T. C., *et al*. (2011) The first identification of lysine malonylation substrates and its regulatory enzyme. *Mol. Cell. Proteomics* **10**. M111.012658
7. Tan, M., Peng, C., Anderson, K. A., Chhoy, P., Xie, Z., Dai, L., Park, J., Chen, Y., Huang, H., Zhang, Y., Ro, J., Wagner, G. R., Green, M. F., Madsen, A. S., Schmiesing, J., *et al*. (2014) Lysine glutarylation is a protein posttranslational modification regulated by SIRT5. *Cell Metab.* **19**, 605–617
8. Chen, Y., Sprung, R., Tang, Y., Ball, H., Sangras, B., Kim, S. C., Falck, J. R., Peng, J., Gu, W., and Zhao, Y. (2007) Lysine propionylation and butyrylation are novel post-translational modifications in histones. *Mol. Cell. Proteomics* **6**, 812–819
9. Zhang, D., Tang, Z., Huang, H., Zhou, G., Cui, C., Weng, Y., Liu, W., Kim, S., Lee, S., Perez-Neut, M., Ding, J., Czyz, D., Hu, R., Ye, Z., He, M., *et al*. (2019) Metabolic regulation of gene expression by histone lactylation. *Nature* **574**, 575–580
10. Weinert, B. T., Iesmantavicius, V., Wagner, S. A., Schölz, C., Gummesson, B., Beli, P., Nyström, T., and Choudhary, C. (2013) Acetyl-phosphate is a critical determinant of lysine acetylation in *E. coli*. *Mol. Cell* **51**, 265–272
11. Starai, V. J., Celic, I., Cole, R. N., Boeke, J. D., and Escalante-Semerena, J. C. (2002) Sir2-dependent activation of acetyl-CoA synthetase by deacetylation of active lysine. *Science* **298**, 2390–2392
12. Starai, V. J., and Escalante-Semerena, J. C. (2004) Identification of the protein acetyltransferase (Pat) enzyme that acetylates acetyl-CoA synthetase in *Salmonella enterica*. *J. Mol. Biol.* **340**, 1005–1012
13. Figlia, G., Willnow, P., and Teleman, A. A. (2020) Metabolites regulate cell signaling and growth via covalent modification of proteins. *Dev. Cell* **54**, 156–170
14. Colak, G., Xie, Z., Zhu, A. Y., Dai, L., Lu, Z., Zhang, Y., Wan, X., Chen, Y., Cha, Y. H., Lin, H., Zhao, Y., and Tan, M. (2013) Identification of lysine succinylation substrates and the succinylation regulatory enzyme CobB in *Escherichia coli*. *Mol. Cell. Proteomics* **12**, 3509–3520
15. Li, P., Zhang, H., Zhao, G. P., and Zhao, W. (2020) Deacetylation enhances ParB-DNA interactions affecting chromosome segregation in *Streptomyces coelicolor*. *Nucleic Acids Res.* **48**, 4902–4914
16. Vazquez, B. N., Thackray, J. K., and Serrano, L. (2017) Sirtuins and DNA damage repair: SIRT7 comes to play. *Nucleus* **8**, 107–115
17. Wei, W., Liu, T., Li, X., Wang, R., Zhao, W., Zhao, G., Zhao, S., and Zhou, Z. (2017) Lysine acetylation regulates the function of the global anaerobic transcription factor FnrL in *Rhodobacter sphaeroides*. *Mol. Microbiol.* **104**, 278–293
18. Han, X., Shen, L., Wang, Q., Cen, X., Wang, J., Wu, M., Li, P., Zhao, W., Zhang, Y., and Zhao, G. (2017) Cyclic AMP inhibits the activity and promotes the acetylation of acetyl-CoA synthetase through competitive binding to the ATP/AMP pocket. *J. Biol. Chem.* **292**, 1374–1384
19. Hong, S. Y., Ng, L. T., Ng, L. F., Inoue, T., Tolwinski, N. S., Hagen, T., and Gruber, J. (2016) The role of mitochondrial non-enzymatic protein acylation in ageing. *PLoS One* **11**, e0168752

20. Ali, I., Conrad, R. J., Verdin, E., and Ott, M. (2018) Lysine acetylation goes global: From epigenetics to metabolism and therapeutics. *Chem. Rev.* **118**, 1216–1252
21. Wang, G., Meyer, J. G., Cai, W., Softic, S., Li, M. E., Verdin, E., Newgard, C., Schilling, B., and Kahn, C. R. (2019) Regulation of UCP1 and mitochondrial metabolism in Brown adipose tissue by reversible succinylation. *Mol. Cell* **74**, 844–857.e847
22. Zhang, H., Li, P., Ren, S., Cheng, Z., Zhao, G., and Zhao, W. (2019) ScCobB2-mediated lysine desuccinylation regulates protein biosynthesis and carbon metabolism in *Streptomyces coelicolor*. *Mol. Cell. Proteomics* **18**, 2003–2017
23. Wagner, G. R., and Payne, R. M. (2013) Widespread and enzyme-independent Nε-acetylation and Nε-succinylation of proteins in the chemical conditions of the mitochondrial matrix. *J. Biol. Chem.* **288**, 29036–29045
24. Sabari, B. R., Zhang, D., Allis, C. D., and Zhao, Y. (2017) Metabolic regulation of gene expression through histone acylations. *Nat. Rev. Mol. Cel. Biol.* **18**, 90–101
25. Kosono, S., Tamura, M., Suzuki, S., Kawamura, Y., Yoshida, A., Nishiyama, M., and Yoshida, M. (2015) Changes in the acetylome and succinylome of *Bacillus subtilis* in response to carbon source. *PLoS One* **10**, e0131169
26. Weinert, B. T., Iesmantavicius, V., Moustafa, T., Scholz, C., Wagner, S. A., Magnes, C., Zechner, R., and Choudhary, C. (2014) Acetylation dynamics and stoichiometry in *Saccharomyces cerevisiae*. *Mol. Syst. Biol.* **10**, 716
27. Zhou, H., Finkemeier, I., Guan, W., Tossounian, M. A., Wei, B., Young, D., Huang, J., Messens, J., Yang, X., Zhu, J., Wilson, M. H., Shen, W., Xie, Y., and Foyer, C. H. (2018) Oxidative stress-triggered interactions between the succinyl- and acetyl-proteomes of rice leaves. *Plant Cell Environ.* **41**, 1139–1153
28. Gaviard, C., Broutin, I., Cosette, P., Dé, E., Jouenne, T., and Hardouin, J. (2018) Lysine succinylation and acetylation in *Pseudomonas aeruginosa*. *J. Proteome Res.* **17**, 2449–2459
29. Pan, J., Chen, R., Li, C., Li, W., and Ye, Z. (2015) Global analysis of protein lysine succinylation profiles and their overlap with lysine acetylation in the marine bacterium *Vibrio parahemolyticus*. *J. Proteome Res.* **14**, 4309–4318
30. Mikulik, K., Felsberg, J., Kudrnacova, E., Bezouskova, S., Setinova, D., Stodulkova, E., Zidkova, J., and Zidek, V. (2012) CobB1 deacetylase activity in *Streptomyces coelicolor*. *Biochem. Cell Biol.* **90**, 179–187
31. Huang, D. W., Sherman, B. T., Tan, Q., Kir, J., Liu, D., Bryant, D., Guo, Y., Stephens, R., Baseler, M. W., Lane, H. C., and Lempicki, R. A. (2007) DAVID Bioinformatics Resources: Expanded annotation database and novel algorithms to better extract biology from large gene lists. *Nucleic Acids Res.* **35**, W169–175
32. Jones, P., Binns, D., Chang, H. Y., Fraser, M., Li, W., McAnulla, C., McWilliam, H., Maslen, J., Mitchell, A., Nuka, G., Pesseat, S., Quinn, A. F., Sangrador-Vegas, A., Scheremetjew, M., Yong, S. Y., *et al*. (2014) InterProScan 5: Genome-scale protein function classification. *Bioinformatics* **30**, 1236–1240
33. Chou, M. F., and Schwartz, D. (2011) Biological sequence motif discovery using motif-x. *Curr. Protoc. Bioinformatics*
34. Colaert, N., Helsens, K., Martens, L., Vandekerckhove, J., and Gevaert, K. (2009) Improved visualization of protein consensus sequences by iceLogo. *Nat. Methods* **6**, 786–787
35. Rajaram, S., and Oono, Y. (2010) NeatMap–non-clustering heat map alternatives in R. *BMC bioinformatics* **11**, 45
36. Franceschini, A., Szklarczyk, D., Frankild, S., Kuhn, M., Simonovic, M., Roth, A., Lin, J., Minguez, P., Bork, P., von Mering, C., and Jensen, L. J. (2013) STRING v9.1: Protein-protein interaction networks, with increased coverage and integration. *Nucleic Acids Res.* **41**, D808–815
37. Su, G., Morris, J. H., Demchak, B., and Bader, G. D. (2014) Biological network exploration with Cytoscape 3. *Curr. Protoc. Bioinformatics* **47**, 11–24
38. Bader, G. D., and Hogue, C. W. (2003) An automated method for finding molecular complexes in large protein interaction networks. *BMC Bioinformatics* **4**, 2
39. Bentley, S. D., Chater, K. F., Cerdeno-Tarraga, A. M., Challis, G. L., Thomson, N. R., James, K. D., Harris, D. E., Quail, M. A., Kieser, H., Harper, D., Bateman, A., Brown, S., Chandra, G., Chen, C. W., Collins, M., *et al*. (2002) Complete genome sequence of the model actinomycete *Streptomyces coelicolor* A3(2). *Nature* **417**, 141–147
40. Cao, J., Wang, T., Wang, Q., Zheng, X., and Huang, L. (2019) Functional insights into protein acetylation in the hyperthermophilic archaeon *Sulfolobus islandicus*. *Mol. Cell. Proteomics* **18**, 1572–1587
41. Yang, Y., Tong, M., Bai, X., Liu, X., Cai, X., Luo, X., Zhang, P., Cai, W., Vallee, I., Zhou, Y., and Liu, M. (2017) Comprehensive proteomic analysis of lysine acetylation in the foodborne pathogen *Trichinella spiralis*. *Front. Microbiol.* **8**, 2674
42. Liu, F., Yang, M., Wang, X., Yang, S., Gu, J., Zhou, J., Zhang, X. E., Deng, J., and Ge, F. (2014) Acetylome analysis reveals diverse functions of lysine acetylation in *Mycobacterium tuberculosis*. *Mol. Cell. Proteomics* **13**, 3352–3366
43. Yu, H., Diao, H., Wang, C., Lin, Y., Yu, F., Lu, H., Xu, W., Li, Z., Shi, H., Zhao, S., Zhou, Y., and Zhang, Y. (2015) Acetylproteomic analysis reveals functional implications of lysine acetylation in human spermatozoa (sperm). *Mol. Cell. Proteomics* **14**, 1009–1023
44. Xiong, Y., Peng, X., Cheng, Z., Liu, W., and Wang, G. L. (2016) A comprehensive catalog of the lysine-acetylation targets in rice (Oryza sativa) based on proteomic analyses. *J. Proteomics* **138**, 20–29
45. Lv, Y. (2017) Proteome-wide profiling of protein lysine acetylation in *Aspergillus flavus*. *PLoS One* **12**, e0178603
46. Lv, B., Yang, Q., Li, D., Liang, W., and Song, L. (2016) Proteome-wide analysis of lysine acetylation in the plant pathogen *Botrytis cinerea*. *Sci. Rep.* **6**, 29313
47. Wang, Y., Wang, F., Bao, X., and Fu, L. (2019) Systematic analysis of lysine acetylome reveals potential functions of lysine acetylation in *Shewanella baltica*, the specific spoilage organism of aquatic products. *J. Proteomics* **205**, 103419
48. Vizcaino, J. A., Csordas, A., Del-Toro, N., Dianes, J. A., Griss, J., Lavidas, I., Mayer, G., Perez-Riverol, Y., Reisinger, F., Ternent, T., Xu, Q. W., Wang, R., and Hermjakob, H. (2016) 2016 update of the PRIDE database and its related tools. *Nucleic Acids Res.* **44**, 11033
49. Baker, P. R., and Chalkley, R. J. (2014) MS-viewer: A web-based spectral viewer for proteomics results. *Mol. Cell. Proteomics* **13**, 1392–1396